INL/CON-22-66067-Revision-0

Sockeye Heat Pipe Analysis Code Verification and Validation

March 2022

Joshua E Hansel, Lise Cecile Madeleine Charlot

Changing the World's Energy Future

INL is a U.S. Department of Energy National Laboratory operated by Battelle Energy Alliance, LLC

INL/CON-22-66067-Revision-0

Sockeye Heat Pipe Analysis Code Verification and Validation

Joshua E Hansel, Lise Cecile Madeleine Charlot

March 2022

Idaho National Laboratory
Idaho Falls, Idaho 83415

http://www.inl.gov

Prepared for the
U.S. Department of Energy
Under DOE Idaho Operations Office
Contract DE-AC07-05ID14517

The 19th International Topical Meeting on Nuclear Reactor Thermal Hydraulics (NURETH-19) Log nr.: 36359
Brussels, Belgium, March 6 - 11, 2022

SOCKEYE HEAT PIPE ANALYSIS CODE VERIFICATION AND VALIDATION

Joshua Hansel and Lise Charlot
Idaho National Laboratory
1955 N Fremont Ave, Idaho Falls, ID 83415
joshua.hansel@inl.gov; lise.charlot@inl.gov

ABSTRACT

Some of the most promising microreactor designs currently under development utilize heat pipe technology to transfer heat from the reactor core to the secondary side heat exchanger, due to the technology's compactness, efficiency, passivity, and reliability. Sockeye is an engineering-scale heat pipe tool developed under the Nuclear Energy Advanced Modeling and Simulation Program to be used for the design and safety analysis of microreactors. Sockeye's core capability lies in a 1D, two-phase, compressible flow model, used to simulate the working fluid inside the heat pipe. Sockeye is built on the Multiphysics Object-Oriented Simulation Environment framework, which allows for seamless multiphysics coupling with other Nuclear Energy Advanced Modeling and Simulation tools and can thus be used in a full-scale simulation of a microreactor assembly, which can include hundreds of heat pipes. This paper presents some initial verification and validation assessments performed for Sockeye. We demonstrate good agreement between Sockeye's numerical results and steady-state analytic solutions for velocity and pressure drop, with differences attributable to the underlying assumptions made by the analytic solutions. We also show that Sockeye reproduces analytic predictions of key operational limits, such as the capillary limit and the sonic limit. Finally, we compare Sockeye results to experimental data for the SAFE-30 heat pipe module test.

KEYWORDS
Heat pipe technology, verification and validation, Sockeye

1. INTRODUCTION

Heat pipes are very efficient, passive, compact, and reliable heat transfer devices operating on two-phase flow with phase change, which have been used in a variety of applications, such as electronics cooling, oil pipelines, air conditioning, and space exploration [1, 2]. In recent years, these devices have been of interest for use in microreactor designs. The Nuclear Energy Advanced Modeling and Simulation (NEAMS) Program is currently developing Sockeye, an engineering-scale heat pipe application, as part of a set of tools for the design and analysis of small modular reactors. Sockeye was introduced in [3], which featured several numerical demonstrations. This work features some additional verification and validation studies that have been performed for Sockeye. It also introduces a simplified heat pipe model based on heat conduction, which was not given in [3]. The concept of modeling a heat pipe using heat conduction equations is not novel (see [4, 5]), but this work features a novel technique for dynamically adjusting to heat pipe limitations.

This paper is organized as follows: Section 2 gives a brief description of the models used in Sockeye, Section 3 gives the results of some verification and validation test problems, and Section 4 gives conclusions.

2. MODELS

Sockeye offers two main simulation capabilities. The first, described in Section 2.1, is a 1D, 2-phase, compressible flow model for the working fluid that can be coupled to 2D heat conduction in the heat pipe wall. The second, described in Section 2.2, is a 2D heat conduction model that approximates the heat pipe vapor core as a superconducting medium.

2.1. Flow Model

Sockeye's primary simulation capability is a 1D, 2-phase, compressible flow model for the working fluid, which can be coupled to 2D heat conduction in the heat pipe wall. This model is described in detail in [3] but is briefly summarized here for convenience.

Sockeye's flow model is adapted from a two-phase flow model derived using the discrete equation method [6]. Both the liquid phase and vapor phase are assumed to be governed by the Euler equations of gas dynamics. Note that viscous effects are considered via volumetric source terms. An averaging procedure yields a system of seven partial differential equations:

$$\frac{\partial \mathbf{U}}{\partial t} + \frac{\partial \mathbf{F}(\mathbf{U})}{\partial x} + \mathbf{B}(\mathbf{U}) \odot \frac{\partial \boldsymbol{\alpha}(\mathbf{U})}{\partial x} = \mathbf{S}(\mathbf{U}) \,, \tag{1}$$

$$\mathbf{U} = \begin{bmatrix} \alpha_\ell A \\ \alpha_\ell \rho_\ell A \\ \alpha_\ell \rho_\ell u_\ell A \\ \alpha_\ell \rho_\ell E_\ell A \\ \alpha_v \rho_v A \\ \alpha_v \rho_v u_v A \\ \alpha_v \rho_v E_v A \end{bmatrix} \quad \mathbf{F} = \begin{bmatrix} 0 \\ \alpha_\ell \rho_\ell u_\ell A \\ \alpha_\ell (\rho_\ell u_\ell^2 + p_\ell) A \\ \alpha_\ell u_\ell (\rho_\ell E_\ell + p_\ell) A \\ \alpha_v \rho_v u_v A \\ \alpha_v (\rho_v u_v^2 + p_v) A \\ \alpha_v u_v (\rho_v E_v + p_v) A \end{bmatrix} \quad \mathbf{B} = \begin{bmatrix} u_{\text{int}} A \\ 0 \\ -p_{\text{int}} A \\ -p_{\text{int}} u_{\text{int}} A \\ 0 \\ -p_{\text{int}} A \\ -p_{\text{int}} u_{\text{int}} A \end{bmatrix} \quad \boldsymbol{\alpha} = \begin{bmatrix} \alpha_\ell \\ \alpha_\ell \\ \alpha_\ell \\ \alpha_\ell \\ \alpha_v \\ \alpha_v \\ \alpha_v \end{bmatrix} .$$

The source vector $\mathbf{S}(\mathbf{U})$ is not detailed here but includes contributions from the following effects:

- Gravity
- Wall heat transfer
- Interfacial heat transfer
- Wall boiling
- Interfacial mass transfer
- Wall friction
- Interfacial friction
- Form loss
- Pressure relaxation

For a detailed description of the source terms, see [3].

For this work, we only consider cases where the working fluid is completely melted.

2.2. Conduction Model

After the startup phase of a heat pipe, a heat pipe can be idealized as a solid cylinder with a very high thermal conductivity, thus ignoring its internal mechanisms, which can be difficult to model. Many researchers have used this analogy to model heat pipes because of its relative simplicity and its ability to accurately capture thermal response in many cases [4, 5]. The idea is simply to solve the heat conduction equation in 2D or 3D and use thermal properties that yield a rod of superconductivity.

The heat conduction equation is expressed as follows:

$$\rho c_p \frac{\partial T}{\partial t} - \nabla \cdot (k \nabla T) = 0 \,, \tag{2}$$

where ρ is density, c_p is specific heat capacity, k is thermal conductivity, and T is temperature. This equation is discretized using the continuous finite element method by multiplying by a trial function ϕ_i, integrating over the domain Ω, and then integrating by parts to get an integral on the boundary Γ:

$$\int_\Omega \rho c_p \frac{\partial T}{\partial t} \phi_i d\Omega + \int_\Omega k \nabla T \cdot \nabla \phi_i d\Omega = \int_\Gamma q \phi_i d\Gamma = 0 \,, \tag{3}$$

where $q \equiv k \nabla T \cdot \mathbf{n}$ is heat flux normal to the boundary, with the convention that a positive value corresponds to heat being transferred from the environment to the domain.

To take the effective heat conduction approach, one can either use thermal properties averaged over the entire cross section of the heat pipe, or one can use different thermal properties in different radial regions. Sockeye takes the latter approach, as it offers a more accurate temperature distribution. Table I summarizes the different regions and different thermal properties used in each region.

Table I. Thermal properties in each radial region for Sockeye's conduction model

Radial Region	ρ	c_p	k
Cladding	ρ_{clad}	$c_{p,\text{clad}}$	k_{clad}
Wick/Annulus	$\rho_{\text{wick/ann}}$	$c_{p,\text{wick/ann}}$	$k_{\text{wick/ann}}$
Core	ρ_v	$c_{p,v}$	k_{core}

In the cladding region, the thermal properties are equal to the thermal properties of the cladding material, and in the wick/annulus region, the thermal properties are equal to volume-weighted averages of the constituent properties of the liquid phase and wick structure:

$$y_{\text{wick/ann}} = \varphi y_\ell + (1 - \varphi) y_{\text{wick}} \,, \tag{4}$$

where φ is the porosity of the entire wick/annulus region.

In the vapor core region, the density and specific heat capacity are those of the vapor phase of the working fluid. The thermal conductivity, however, is a high value to reflect the high effective thermal conductivity of heat pipe operation.

An improvement of this approach makes this thermal conductivity dynamic with the solution, since this high effective thermal conductivity is only realized when the throughput of the heat pipe is not being limited. For example, at lower temperatures, the sonic limitation (see Section 3.3) severely limits the rate at which heat can move through the vapor core. This dynamic behavior can be achieved by scaling the thermal conductivity in the core at each time step:

$$k_{\text{core}}^{(n+1)} = \beta^{(n)} k_{\text{core}}^{(n)} \,, \tag{5}$$

where (n) is a time step index and the scaling factor is defined as $\beta = \dot{Q}_{\text{max}}/\dot{Q}_{\text{core}}$, with $\dot{Q}_{\text{max}}$ being the most restrictive heat transfer limit and $\dot{Q}_{\text{core}}$ being the rate of heat through the evaporator exit in the vapor core. Denoting $T_n \equiv \nabla T \cdot \mathbf{n}$, where $\mathbf{n}$ is the direction pointing *away* from the evaporator, and $\overline{T_n}$ to be the average of T_n over the evaporator exit surface, the core heat rate is expressed as

$$\dot{Q}_{\text{core}} = -k_{\text{core}} \overline{T_n} A_{\text{core}} \,, \tag{6}$$

where A_{core} is the cross-sectional area of the vapor core. Assuming $\overline{T_n}^{(n+1)} \approx \overline{T_n}^{(n)}$, the definition given by Eq. (5) effectively adjusts the heat rate through the vapor core according to the previous time step's heat rate limit: $\dot{Q}_{\text{core}}^{(n+1)} = \dot{Q}_{\text{max}}^{(n)}$. Note that, in practice, k_{core} is constrained to be within some upper and lower bounds.

3. RESULTS

3.1. Steady State Solutions

In [3], a pair of test problems were investigated for comparing Sockeye results with analytic steady-state solutions for the liquid and vapor pressure drops and velocities. In these test problems, an identical heat pipe is subjected to two different heating configurations, one having a single condenser end and the other having two condenser ends, with a central evaporator region. Here, these problems are repeated but modified to increase the pressure drop in the liquid phase. The heat pipe parameters are the same as those for the single-ended heat pipe described in [3], except that the permeability was decreased by a factor of 10 to $5 \cdot 10^{-11}$ m^2 and the pore diameter was reduced to increase the capillary limit and accommodate the larger pressure drops. The simulation parameters are kept the same: 100 uniform elements are used along the length, and a BDF2 time integration with an adaptive time step size is used and run until steady.

The velocity profiles are identical to those presented in [3], matching the analytic solutions, and are not repeated here. For the vapor phase, Cotter's theory [7] was used to derive an analytic solution for the pressure profile, and Darcy's law was used to analyze the pressure drop [2] in the liquid phase. Fig. 1a shows the comparison of the analytic vapor pressure drops with the vapor pressure solution from Sockeye, as well as the saturation pressure at the vapor temperature, for the single-ended configuration. As in [3], the vapor pressure drops within each region match analytical solutions very well, but jumps between the regions are present and are attributed to the sharp temperature changes between the regions, as suggested by the saturation pressure profile. These non-isothermal effects are neglected in the analytic solution. Fig. 1b shows the comparison of the analytic liquid pressure drops with the liquid pressure solution from Sockeye for the single-ended configuration, showing excellent agreement.

3.2. Capillary Limit

The circulation of the working fluid in a heat pipe relies on the capillary pumping ability of its wick structure. When the capillary forces are insufficient to sustain the circulation of the working fluid, the

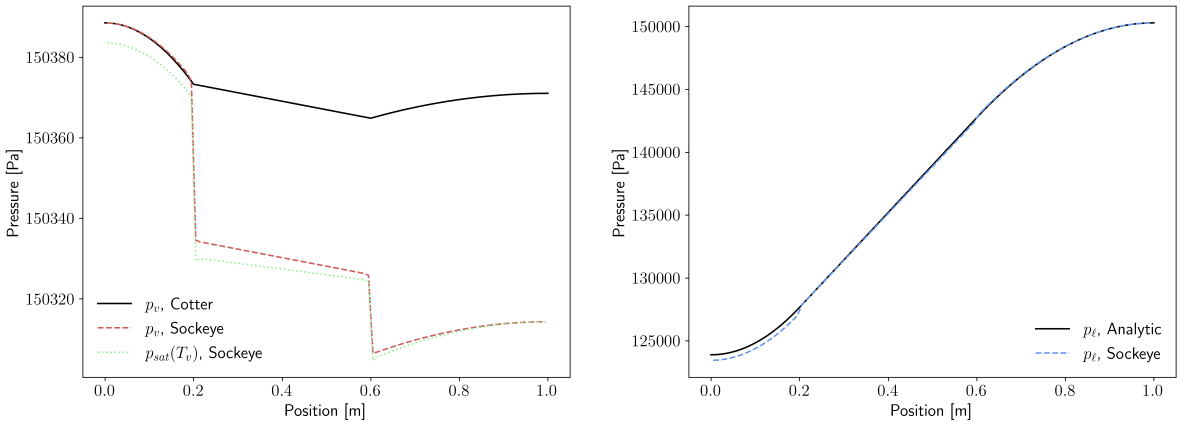

(a) Vapor pressure drop. **(b) Liquid pressure drop.**

Figure 1. Comparison of liquid and vapor pressure drops with analytic solutions for the single-ended configuration.

liquid phase of the working fluid in the evaporator region is depleted over time due to the evaporation rate exceeding the liquid return rate, leading to a condition referred to as dry-out, which represents a heat pipe failure requiring intervention. The minimum heat rate at which this occurs for a given operating temperature is referred to as the capillary limit, $\dot{Q}_{\text{cap}}$.

To derive an analytic relation for this limit, the pressure drops around the heat pipe circuit are summed and compared to the maximum capillary pressure that the wick can provide. A commonly used expression for the capillary limit heat rate from this analysis appears as follows [1, 2]:

$$\dot{Q}_{\text{cap}}(T) = \frac{\rho_\ell(T)\sigma(T)h_{\text{lat}}(T)}{\mu_\ell(T)} \frac{KA_\ell}{L_{\text{eff}}} \left(\frac{2}{R_{\text{eff}}} - \frac{\rho_\ell(T)gL_{\text{hp}}}{\sigma(T)} \sin\theta \right) , \tag{7}$$

where ρ_ℓ is the liquid density, μ_ℓ is the liquid dynamic viscosity, σ is the surface tension, h_{lat} is the latent heat of vaporization, K is the permeability of the liquid channel, A_ℓ is the cross-sectional area of the liquid channel, R_{eff} is the effective pore radius, g is the acceleration due to gravity, θ is the heat pipe inclination angle ($\theta = 0$ corresponds to horizontal, $\theta = -\frac{\pi}{2}$ corresponds to gravity-assisted, and $\theta = \frac{\pi}{2}$ corresponds to gravity-adverse), L_{hp} is the *total* length of the heat pipe, and L_{eff} is the *effective* length of the heat pipe shown here,

$$L_{\text{eff}} = \frac{1}{2}L_{\text{evap}} + L_{\text{adia}} + \frac{1}{2}L_{\text{cond}} , \tag{8}$$

where L_{evap} is the evaporator length, L_{adia} is the adiabatic length, and L_{cond} is the condenser length.

In this study, the capillary limit is investigated at a number of different operating temperatures. One Sockeye run is performed for each operating temperature, and the procedure for each run is as follows. First, a steady state at low power is established, starting from a given initial temperature. Then, the power is slowly increased until the capillary limit is detected via the following criteria at any axial position, at which point the simulation is terminated:

$$\alpha_v > \alpha_v^{\text{wick,i,max}} , \tag{9}$$

where $\alpha_v^{\text{wick,i,max}}$ corresponds to the void fraction such that the liquid-vapor interface is radially located on the inner surface of the wick, with maximum curvature. This criteria is justified by the fact that this maximum curvature corresponds to the maximum capillary pressure; if the interface recedes into the wick past this point, it implies that the capillary pressure was not able to sustain the interface. It should be noted that the termination criteria used in this study is not a default behavior in Sockeye; ordinarily, a simulation will proceed until either the end time is reached or a numerical failure is encountered, such as a divergent nonlinear solve.

Fig. 2 shows the average temperature and corresponding power at which each run terminated and compares these points to the analytic curve for the capillary limit, indicating decent agreement. Sockeye is able to capture the decrease in capillary limit with increasing temperature, though its capillary limit values are roughly 50 W lower than the analytic values in the high temperature range.

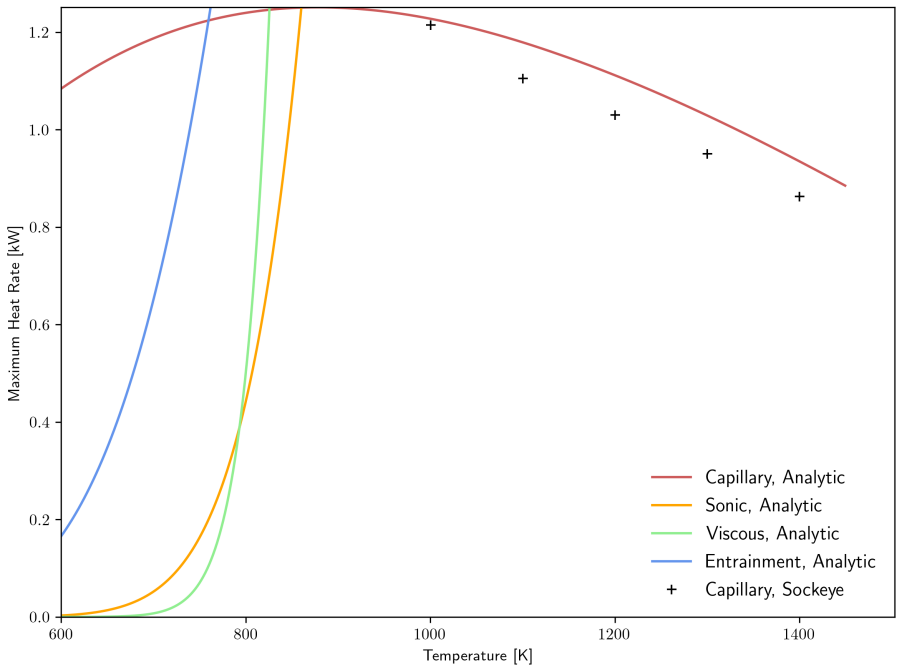

Figure 2. Comparison of capillary limit computed using Sockeye to analytic solution.

3.3. Sonic Limit

During a heat pipe startup, compressibility effects in the vapor phase can lead to a heat transfer limitation known as the sonic limit. The vapor core in a heat pipe has been likened to flow in a convergent-divergent nozzle, with the evaporator region corresponding to the convergent portion and the condenser corresponding to the divergent portion. For the case of a convergent-divergent nozzle, the varying cross section leads to axial velocity changes, whereas for the heat pipe case, cumulative mass injection and extraction lead to velocity changes. For a converging-diverging nozzle, as the ratio of the upstream pressure to the downstream pressure increases, the velocity increases until the flow becomes sonic at the throat, at which point the flow becomes “choked”; that is, further decreases in the downstream pressure relative to the upstream pressure do not cause further changes upstream of the throat. However, note that, downstream of the throat, supersonic conditions may result. The case of a heat pipe is not quite so simple since there are also heat transfer contributions to the pressure gradient. The sonic point in a heat pipe is

often located at the evaporator exit, but its location ultimately depends on other factors, such as friction and heat transfer. For example, sometimes the sonic point may occur in the condenser due to the pressure drop from the temperature decrease there.

A common analytic expression for this heat rate limit can be derived by assuming the vapor is an ideal gas and neglecting friction [1, 2]:

$$\dot{Q}_{\text{sonic}}(T) = \frac{\rho_v(T) c_v(T) h_{\text{lat}}(T) A_v}{\sqrt{2(\gamma_v + 1))}}\,, \tag{10}$$

where ρ_v, c_v, h_{lat}, and γ_v are the vapor density, sound speed, latent heat of vaporization, and ratio of specific heats (c_p/c_v), respectively, all evaluated at the evaporator end-cap temperature T and corresponding saturation pressure, and A_v is the cross-sectional area of the vapor channel.

In this study, we show how Sockeye can be used to generate the curve $\dot{Q}_{\text{sonic}}(T)$. First, heat pipe design parameters were chosen such that no other operational limit should interfere with this analysis (i.e., the heat pipe is designed such that the sonic limit is the most restrictive heat transfer limit). For example, the permeability was set to a relatively high value to raise the capillary limit. To give consistency with the analytic relation, the friction in the vapor core is neglected.

Four Sockeye runs were made, each at a different uniform initial temperature: 800 K, 850 K, 900 K, and 950 K. Whenever power is applied to the heat pipe, power is added and removed in equal amounts such that there is never any net heat transfer into the heat pipe, thus ensuring that the final temperatures are in the vicinity of the initial temperatures. Note that for these conditions, the heat pipe operation is not yet isothermal, so the temperature of interest, the evaporator end-cap temperature, can be noticeably higher than the initial temperature. In each run, a steady operation is initially established with 100 W, at which point power begins to ramp up. Power continues to ramp linearly until the Mach number is greater than or equal to one at any point in the pipe, at which point the simulation is terminated. Upon termination, the current power level and evaporator end-cap temperature are recorded. Fig. 3 plots the temperature and power for each run against the analytic sonic limit given by Eq. (10), which demonstrates excellent agreement, despite that a real equation of state was used instead of an ideal gas equation of state, which was assumed in the derivation of the analytic sonic limit.

3.4. SAFE-30 Heat Pipe Module Experiment

The SAFE-30 heat pipe module experiment tested the performance of a heat pipe module for non-nuclear simulations of the SAFE-30 reactor [8]. The experimental setup consisted of a single, stainless steel, sodium heat pipe coupled to four "fuel tubes," heated by cartridge heaters. Table II summarizes the heat pipe design parameters. Note that a representative value was used for wick permeability, since this information was not given in [8]. The heat pipe module was enclosed in a vacuum chamber in a room-temperature environment. Power was supplied to the four cartridge heaters, and the heat pipe was passively cooled via radiation.

The experiment ran for 7 hours (25,000 seconds), and in [3], the experiment was simulated from $t = 8000$ s to $t = 9575$ s. Shortly after the end time, the simulation was terminated due to numerical issues associated with the appearance of the condenser pool (due to the complete disappearance of the vapor phase). An updated flow model is used in this work, along with a temperature-dependent contact angle, which allowed the simulation to run past the original termination time; in this work, the simulation starts at $t = 7,500$ s and ends at $t = 18,000$ s, shortly after which the simulation fails. The exact reason for the failure has not

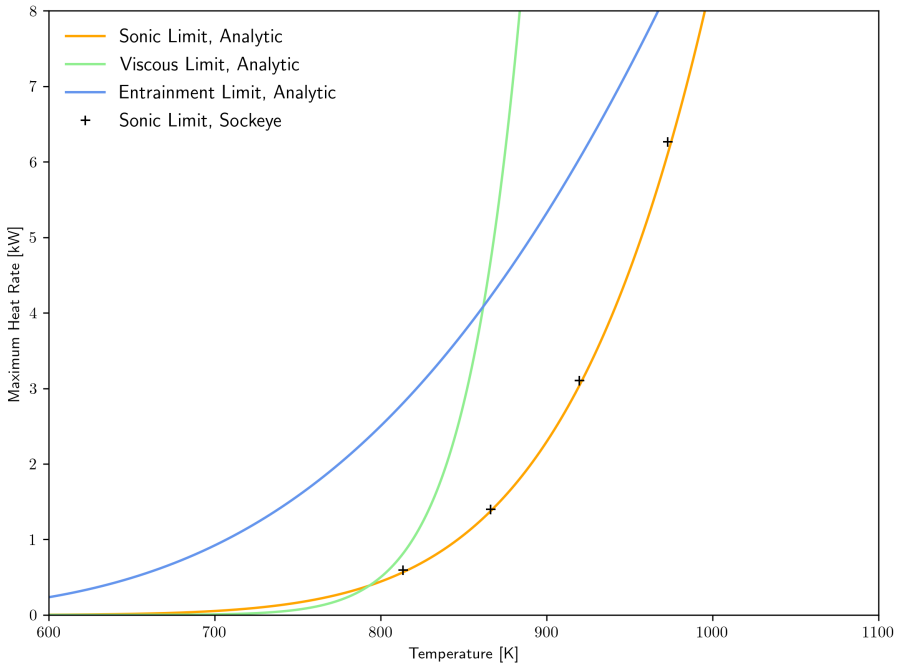

Figure 3. Comparison of sonic limit computed using Sockeye to analytic solution.

Table II. SAFE-30 heat pipe description

Parameter	Value
Working fluid	Sodium
Working fluid mass, m	0.1453 kg
Wick inner diameter, $D_{\text{wick,i}}$	0.0174 m
Wick outer diameter, $D_{\text{wick,o}}$	0.0207 m
Cladding inner diameter, $D_{\text{clad,i}}$	0.0221 m
Cladding outer diameter, $D_{\text{clad,o}}$	0.0254 m
Evaporator length, L_{evap}	0.43 m
Condenser length, L_{cond}	0.77 m
Wick porosity, φ	0.807308741
Pore radius, R_{pore}	47×10^{-6} m
Wick permeability, K	10^{-10} m^2
Orientation	Horizontal

been identified, but the failure is believed to be related to the very low pressures at the minimum operating temperature at the end of the transient, around 450 K, which for reference has a saturation pressure of

roughly 0.0046 Pa. This near-vacuum state has been noted to be a sensitive regime for fluid property look-ups, since small deviations from the saturation state may result in unphysical thermodynamic states.

Sockeye's 1D, two-phase flow model was coupled to 2D heat conduction in the heat pipe cladding. The remainder of the heat pipe module, such as the fuel tubes, are not included in the physical domain; instead, the estimated power from the fuel tubes to the heat pipe is applied as a uniform heat flux on the outer surface of the heat pipe in the evaporator region. The radiative losses were computed using radiative boundary conditions on the outer surface of the heat pipe:

$$q = \epsilon\sigma F(T_\infty^4 - T^4)\,, \tag{11}$$

where q denotes the heat flux to be used in the boundary flux term in Eq. (3), ϵ denotes the emissivity of the surface, σ is the Stefan-Boltzmann constant, F is the view factor, T_∞ is the environment temperature, and T is the surface temperature. In the condenser section, the heat pipe is fully exposed, so $F = 1$, whereas the evaporator section is only partially uncovered due to contact with the fuel tubes containing the cartridge heaters, so $F = 0.25$ is used. The environment temperature for the radiation exchange and surface emissivity from [8] are 296 K and 0.4, respectively.

The input power to the heat pipe from the fuel tubes, $\dot{Q}_{\text{in}}$, is shown in Fig. 4, as well as the heat loss rate, $\dot{Q}_{\text{out}}$, which includes radiative losses from both the condenser section and the exposed portion of the evaporator section. During the ramp up to the maximum power, the heat loss rate lags the heat input rate, whereas during the ramp back down from the maximum power, the situation is reversed.

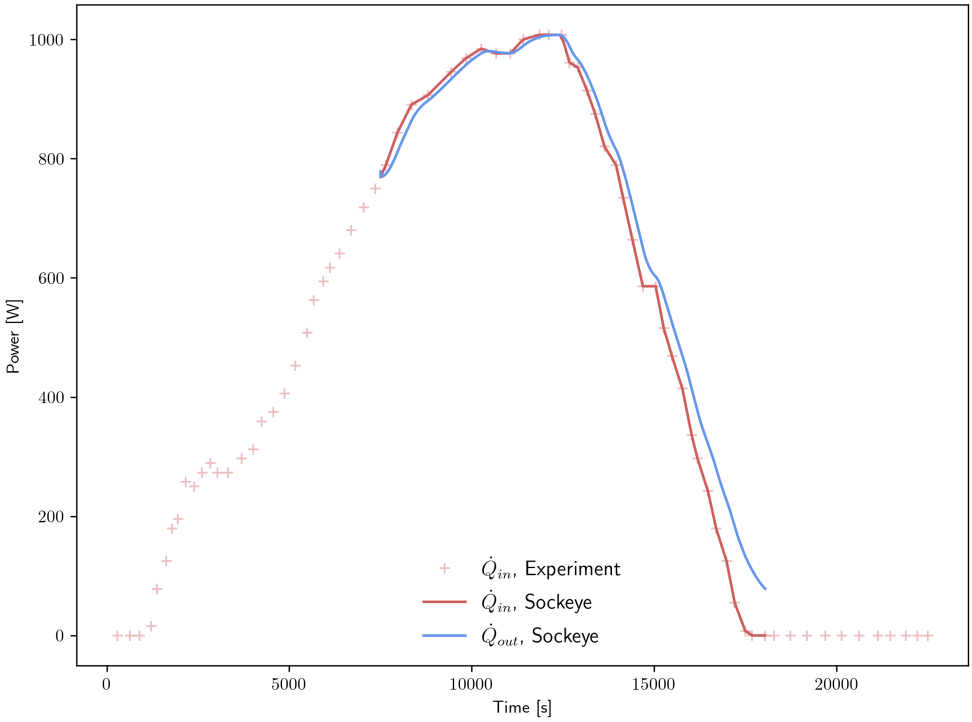

Figure 4. Power transient for SAFE-30 test problem.

Fig. 5 shows the temperature transient for the five thermocouples installed on the heat pipe, whose locations are given in Table III. Generally, the Sockeye temperatures appear to follow the measured

temperatures well. However, near the end of the simulation, the temperatures drop faster than the measured values. The success of reproducing these external temperature measurements depends largely on accurate modeling of the boundary conditions imposed on the heat pipe cladding. From these results, it appears that the boundary conditions need adjustment at lower temperatures. Some possibilities for the discrepancy could be that the emissivity needs dependence on temperature or that the environment itself has heated. Also, it's possible that explicitly modeling the fuel tubes could lead to some improvement, as radiation from the tubes could collide with the condenser section of the heat pipe. Also, the heat capacity of the fuel tubes and heaters themselves are not accounted in this model, which would serve to slow the cooldown of the module. Despite the discrepancies in temperatures at the end of the transient, Sockeye did very well in capturing the onset of the divergence of temperature values in the second half of the simulation, which suggests that the internal heat pipe mechanisms are functioning properly.

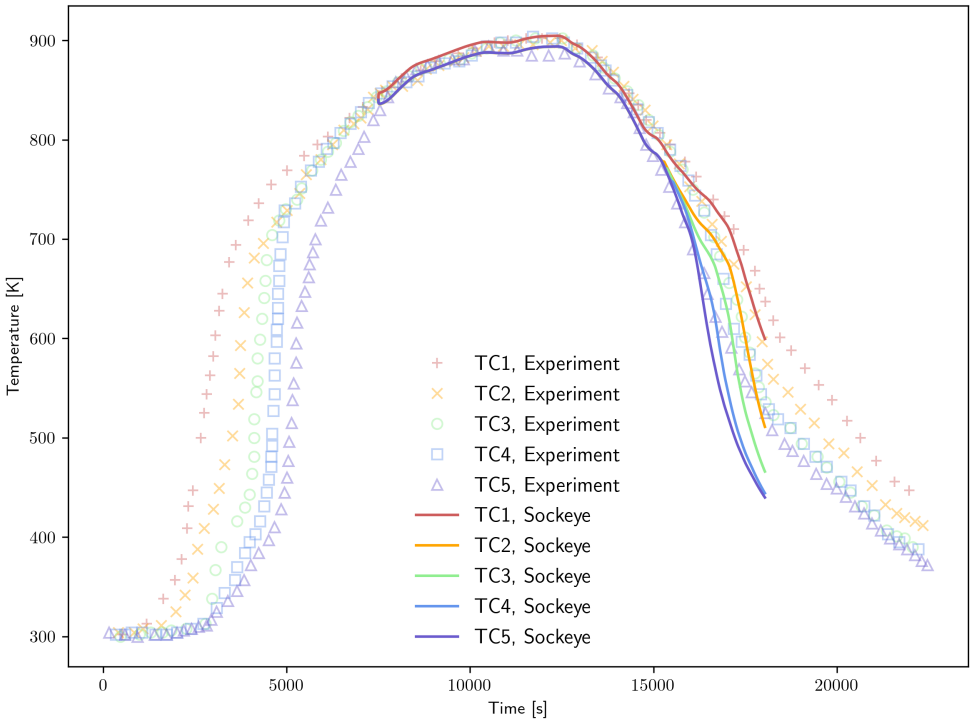

Figure 5. Sockeye flow model temperature transient results for the SAFE-30 test problem.

For comparison, this test problem was also run with the conduction model described in Section 2.2. Unlike the flow model, the conduction model is able to simulate the full length of the experiment, starting at the frozen state, since the conduction model does not attempt any fluid property look-ups other than those on the saturation curve. The transient of k_{core}, which was computed via Eq. (5), is shown in Fig. 6. The allowable range of core thermal conductivity was $k_{\text{core}} \in (10^2 \frac{\text{W}}{\text{m-K}}, 10^7 \frac{\text{W}}{\text{m-K}})$. At the beginning of the transient, the heat rate is limited by the sonic limit until roughly $t = 2500$ s, when the evaporator end-cap temperature has increased enough for the sonic limit to no longer be restrictive. With the continued heating, the temperature, and thus the sonic limit, continues to grow, causing k_{core} to grow as well until it hits its maximum. During the shutdown ramp, the opposite occurs. The resulting temperature transient is shown in Fig. 7. Compared to the experiment, the temperatures follow the transient trend reasonably well but rise faster during startup and fall faster during the shutdown. This is believed to be largely because the latent heat of fusion is not considered in this model. Like the flow model, this simulation would also be

Table III. SAFE-30 thermocouple locations

Name	Distance from Evaporator Endcap
TC1	0.216 m
TC2	0.508 m
TC3	0.711 m
TC4	0.914 m
TC5	1.090 m

improved significantly with a more accurate modeling of the boundary conditions.

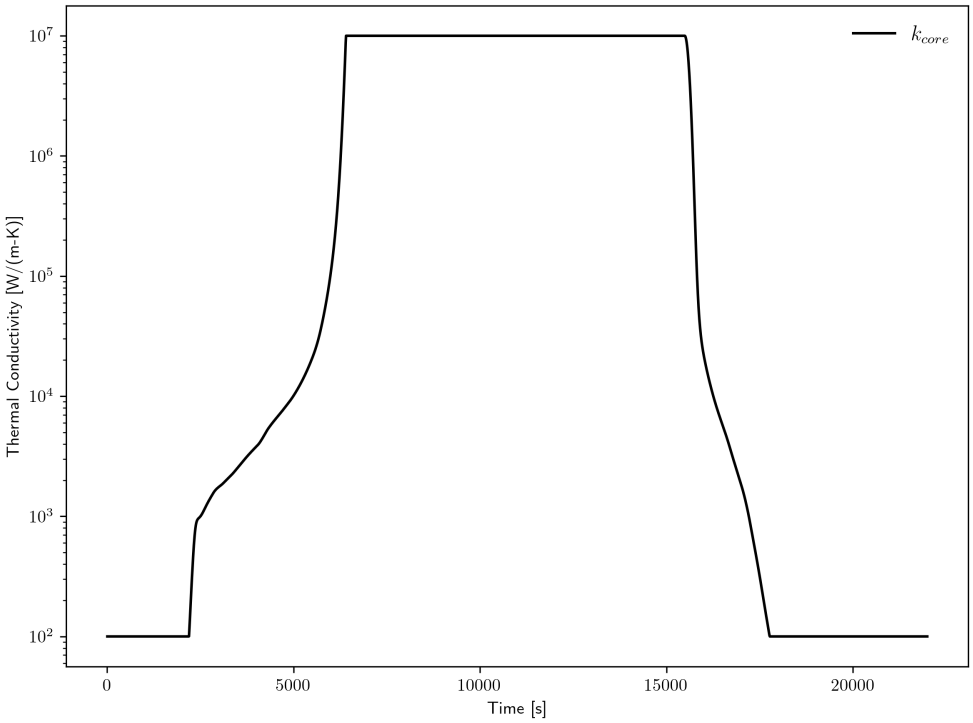

Figure 6. Sockeye conduction model core thermal conductivity transient results for the SAFE-30 test problem.

4. CONCLUSIONS

The heat pipe code Sockeye is currently under development and is concurrently undergoing verification and validation. This work described new validation work performed for Sockeye, as well as improvements to a selection of test problems introduced in [3]. The comparison with analytic steady solutions for the velocities and pressure drops shows excellent agreement with analytic solutions; velocity profiles are visually indistinguishable from the analytic solutions, the liquid pressure drop matches the analytic

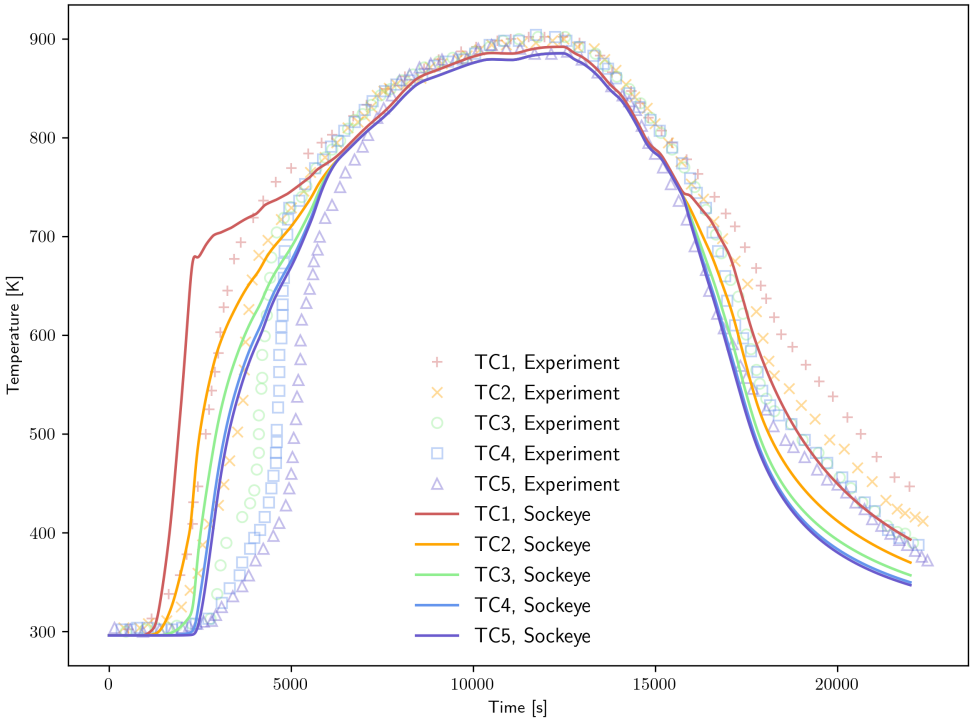

Figure 7. Sockeye conduction model temperature transient results for the SAFE-30 test problem.

solution very well, and the vapor pressure drop matches the analytic solution very well within each region but features jumps between regions due to jumps in vapor temperature, not present in analytic solutions because of their isothermal assumptions. Test problems were created to numerically investigate the capillary and sonic limits using Sockeye at various operating temperatures, and these values were shown to match very well with commonly used analytic expressions for these limits. Finally, a simulation of the SAFE-30 experiment was repeated with recent improvements to Sockeye's flow model, greatly extending the simulated duration of the experiment from previous attempts. Also, a new, simplified, heat pipe model based on heat conduction was introduced and applied to the SAFE-30 test problem, showing good agreement with experimental data but also indicating room for improvement, such as accounting for the latent heat of fusion during heat pipe startup and shutdown. From both SAFE-30 simulations, it was clear that boundary conditions need improvement for more accurate temperature solutions.

Future work on the Sockeye project will include both code development and more verification and validation activities. Heat pipe experiments are underway and will provide various physical measurements, including some measurements internal to the heat pipe [9, 10]. These experiments are being performed in conjunction with a maturing verification and validation plan. Future validation work is planned to be supported by uncertainty quantification for each model, according to uncertainties in heat pipe specifications and experimental configurations.

ACKNOWLEDGMENTS

Sockeye development is being carried out under the auspices of Idaho National Laboratory, a contractor of the U.S. Government under contract number DEAC07-05ID14517. Accordingly, the U.S. Government retains a nonexclusive, royalty-free license to publish or reproduce the published form of this contribution, or allows others to do so, for U.S. Government purposes.

REFERENCES

1. D. A. Reay, P. A. Kew, and R. J. McGlen, *Heat Pipes: Theory, Design and Applications*, Elsevier Ltd., sixth edition, (2014)
2. A. Faghri, *Heat Pipe Science and Technology*, Global Digital Press, second edition, (2016)
3. J. E. Hansel, R. A. Berry, D. Andrs, M. S. Kunick, and R. C. Martineau, "Sockeye: A One-Dimensional, Two-Phase, Compressible Flow Heat Pipe Application," *Nuclear Technology*, **207** (7), pp. 1096–1117 (2021)
4. K. Panda, I. Dulera, and A. Basak, "Numerical Simulation of High Temperature Sodium Heat Pipe for Passive Heat Removal in Nuclear Reactors," *Nuclear Engineering and Design*, **323**, pp. 376–385 (2017)
5. M. Ma et al., "A Pure-Conduction Transient Model for Heat Pipes via Derivation of a Pseudo Wick Thermal Conductivity," *International Journal of Heat and Mass Transfer*, **149**, pp. 119122 (2020)
6. R. A. Berry, R. Saurel, and O. LeMetayer, "The Discrete Equation Method (DEM) for Fully Compressible, Two-Phase Flows in Ducts of Spatially Varying Cross-Section," *Nuclear Engineering and Design*, **240** (11), pp. 3797–3818 (2010)
7. T. Cotter, "Theory of Heat Pipes," LA-3246-MS, Los Alamos National Laboratory (1965)
8. R. S. Reid, J. T. Sena, and A. L. Martinez, "Sodium Heat Pipe Module Test for the SAFE-30 Reactor Prototype," *AIP Conference Proceedings, Albuquerque, New Mexico*, **552** (1), pp. 869–874 (2001)
9. V. Petrov, "NEUP Project 19-17416: Experiments and computations to address the safety case of heat pipe failures in Special Purpose Reactors," Technical abstract, 2019
10. S. Lee, "NEUP Project 20-19735: Experiments for Modeling and Validation of Liquid-Metal Heat Pipe Simulation Tools for Micro-Reactors," Technical abstract, 2020